

Article

Preparation and Characterization of Polymer-Modified Sulphoaluminate-Cement-Based Materials

Xinrui Feng * and Bei Liu

College of Civil Engineering and Architecture, Hainan University, Haikou 570228, China

* Correspondence: fxrgreat@hainanu.edu.cn

Abstract: In situ polymerization of molecular monomers is a novel modification method for cement-based materials, effectively enhancing their properties. An orthogonal test method was employed to optimize the impact of polymers on sulfoaluminate-cement-based materials, incorporating range analysis and variance analysis to investigate the influences of the monomer, initiator, and crosslinker on the compressive strength and flexural strength. A comprehensive scoring method was utilized to determine the optimal polymer content. The modified cement-based materials were characterized through SEM, XRD, and FT-IR tests. The results demonstrated that the monomer significantly influenced the properties of modified cement-based materials. When the monomer content was 5%, the initiator content was 3%, and the crosslinking agent content was 2.5%, the mechanical properties of polymer-modified cement-based materials reached their peak. Characterization experiments revealed that in situ polymerization of molecular monomers led to more compact and compatible modified sulfoaluminate-cement-based material, with an improved organic–inorganic hybrid double network spatial structure that enhanced its structure and mechanical properties.

Keywords: polymer; orthogonal test; sulphoaluminate cement; structural characterization



Citation: Feng, X.; Liu, B. Preparation and Characterization of Polymer-Modified Sulphoaluminate-Cement-Based Materials. *Appl. Sci.* **2024**, *14*, 3366. <https://doi.org/10.3390/app14083366>

Academic Editors: Sara Cattaneo and Manuela Alessandra Scamardo

Received: 18 March 2024

Revised: 15 April 2024

Accepted: 15 April 2024

Published: 16 April 2024



Copyright: © 2024 by the authors. Licensee MDPI, Basel, Switzerland. This article is an open access article distributed under the terms and conditions of the Creative Commons Attribution (CC BY) license (<https://creativecommons.org/licenses/by/4.0/>).

1. Introduction

Polymer-modified cement-based materials are commonly incorporated into cement-based materials in the form of polymers and polymer fibers to form organic–inorganic composite materials, which have the strength of inorganic materials and the flexibility of organic materials. These composites exhibit high strength, wear resistance, corrosion resistance, and other desirable properties [1–4]. However, their uniformity, adhesion, and compatibility with cement-based materials are often poor, leading to insignificant performance improvements [5,6]. For instance, Jin Hesong et al. [7] observed improved frost resistance but no significant enhancement in compressive strength or flexural strength when using polypropylene-fiber-modified cement-based composite materials for dams.

By introducing organic–inorganic hybrid polymerization into cement-based materials, it is possible to synthesize polymers in situ from monomers, thus creating an organic polymer network structure. This process involves simultaneous crosslinking and entangling with the inorganic network structure formed by hydration products of cement, resulting in an organic–inorganic dual network structure. In comparison to the direct addition of polymers, this method offers fuzzy interface adhesion between modified cement-based materials through in situ polymerization, along with a dense and compatible structure that leads to significant performance improvement [8–10]. However, there is currently limited research on the mechanism behind modifying cementitious material through in situ polymerization. Furthermore, most studies focus on single-factor additions rather than comprehensive impacts on material properties using polymers formed via this technique [11–13].

To address the aforementioned deficiencies, this study utilized a polymer consisting of an acrylamide monomer, ammonium persulfate initiator, and N,N'-methylene bisacrylamide crosslinking agent to improve a sulfoaluminate-mud-based material. Sulfoaluminate cement is widely used and cost-effective in marine engineering [14,15]. The experimental results were subjected to orthogonal experiments, range analysis, and variance analysis to determine the optimal level of combination using a comprehensive scoring method. Qualitative, quantitative, and mechanistic analyses of the polymer-modified sulfoaluminate-mud-based materials were conducted through SEM, XRD, and FT-IR tests.

2. Materials and Methods

2.1. Materials and Instruments

The cement used was sulfoaluminate cement, of SAC42.5 grade, provided by Dengdian Group Cement Co., Ltd, Dengfeng, China. Acrylamide, ammonium persulfate, and N,N'-methylene bisacrylamide were all supplied by Shanghai McLean Biochemical Technology Co., Ltd, Shanghai, China.

SEM was utilized to characterize the polymer morphology on a Verios G4 UC field emission scanning electron microscope instrument (Thermo Fisher, Waltham, MA, USA). Polymer structure was conducted on a SmartLab X-ray diffractometer equipment (Rigaku, Osaka, Japan). FTIR analysis was conducted using an FTIR-650 infrared spectrometer (Gangdong, Tianjin, China). The measured wavenumbers ranged from 400 to 4000 cm^{-1} .

2.2. Materials' Preparation

The test specimens were fabricated under controlled laboratory conditions at a temperature of $20\text{ }^{\circ}\text{C} \pm 2\text{ }^{\circ}\text{C}$ and a relative humidity exceeding 50%. These specimens were made into prisms measuring 40 mm \times 40 mm \times 160 mm. According to the design table for orthogonal experiments, precise amounts of initiator and crosslinking agent were accurately weighed before being added into separate solutions containing 50 mL water each. These solutions were then thoroughly stirred. Cement and monomer were introduced into a cement slurry mixer for a duration of 60 s, followed by gentle mixing with water for an additional period of 120 s. During this process, the initiator solution was gradually incorporated first, followed by the crosslinking agent solution. Finally, rapid mixing was performed for another duration of 60 s prior to molding. After undergoing curing in standard room conditions for seven days, performance testing was conducted.

2.3. Orthogonal Experimental Design

Orthogonal experimental design is a kind of experimental design method for multi-factor and multi-level studies. By analyzing the effect and interaction of each factor, the optimal level of combination can be selected [16]. In order to obtain the optimum preparation conditions of modified cement-based materials, orthogonal tests were carried out. Using compressive strength and flexural strength as test indexes, and the monomer, initiator and crosslinker as test factors, the L25 (5^6) orthogonal experimental design table was selected. The orthogonal experimental design factor level table can be found in Table 1.

Table 1. Orthogonal experimental design factor level table.

| Level | Considerations | | |
|-------|----------------|-------------|---------------|
| | Monomer A | Initiator B | Crosslinker C |
| 1 | 1% | 0.80% | 0.50% |
| 2 | 3% | 1.60% | 1% |
| 3 | 5% | 2.40% | 1.50% |
| 4 | 7% | 3.20% | 2% |
| 5 | 9% | 4.00% | 2.50% |

2.4. Mechanical Performance Testing

The compressive strength and flexural strength were tested. The loading speed for the flexural strength test of cement gel material was $0.05 \text{ KN/s} \pm 0.005 \text{ KN/s}$. After the flexural strength test of three test pieces formed in each group was conducted, the compressive strength test was conducted immediately. The loading speed was $2.4 \text{ KN/s} \pm 0.2 \text{ KN/s}$, and the data processing of compressive strength and flexural strength was conducted according to the specification requirements [17].

2.5. Structural Characterization

The 7-day-old acrylamide in situ-modified cement gel sample was soaked in absolute ethanol for 48 h to stop hydration, and then dried in a 40°C vacuum drying oven for 24 h. After gold spraying, the dried sample was taken for field emission scanning electron microscope analysis. The sample was ground into powder in an agate grinding bowl and analyzed by X-ray diffraction. The scanning range was $5\text{--}80^\circ\text{C}$ and the scanning speed was $5^\circ/\text{min}$. The sample was tested by Fourier infrared spectroscopy with the wavenumber ranging from 400 to 4000 cm^{-1} .

3. Results and Discussion

3.1. Analysis of Orthogonal Experimental Results

Mechanical properties are crucial characteristics of cement-based materials. In this study, compressive strength and flexural strength were selected as the key mechanical properties of materials. According to the orthogonal design, the 7-day flexural strength and compressive strength of polymer-modified cement-based materials were determined. The results are shown in Table 2, and variance analysis and range analysis were conducted to assess the test results. Furthermore, the comprehensive scoring method was employed to identify the optimal level of combination in the experiment.

Table 2. Orthogonal test results.

| Test No. | A | B | C | Amount of Test Material | | | | | Flexural Strength (MPa) | Compressive Strength (MPa) |
|----------|---|---|---|-------------------------|------------|-------------|----------------|------------------|-------------------------|----------------------------|
| | | | | Water (g) | Cement (g) | Monomer (g) | Initiators (g) | Crosslinkers (g) | | |
| 1 | 1 | 1 | 1 | 630 | 1400 | 14 | 0.112 | 0.07 | 3.96 | 34.71 |
| 2 | 1 | 2 | 3 | 630 | 1400 | 14 | 0.224 | 0.21 | 3.54 | 35.23 |
| 3 | 1 | 3 | 5 | 630 | 1400 | 14 | 0.336 | 0.35 | 4.68 | 36.91 |
| 4 | 1 | 4 | 2 | 630 | 1400 | 14 | 0.448 | 0.14 | 4.61 | 36.87 |
| 5 | 1 | 5 | 4 | 630 | 1400 | 14 | 0.56 | 0.28 | 4.22 | 32.03 |
| 6 | 2 | 1 | 5 | 630 | 1400 | 42 | 0.336 | 1.05 | 4.74 | 36.53 |
| 7 | 2 | 2 | 2 | 630 | 1400 | 42 | 0.672 | 0.42 | 3.63 | 33.58 |
| 8 | 2 | 3 | 4 | 630 | 1400 | 42 | 1.008 | 0.84 | 5.34 | 36.03 |
| 9 | 2 | 4 | 1 | 630 | 1400 | 42 | 1.344 | 0.21 | 4.24 | 36.88 |
| 10 | 2 | 5 | 3 | 630 | 1400 | 42 | 1.68 | 0.63 | 3.67 | 30.83 |
| 11 | 3 | 1 | 4 | 630 | 1400 | 70 | 0.56 | 1.4 | 4.26 | 34.15 |
| 12 | 3 | 2 | 1 | 630 | 1400 | 70 | 1.12 | 0.35 | 4.49 | 34.71 |
| 13 | 3 | 3 | 3 | 630 | 1400 | 70 | 1.68 | 1.05 | 4.13 | 34.19 |
| 14 | 3 | 4 | 5 | 630 | 1400 | 70 | 2.24 | 1.75 | 5.40 | 38.05 |
| 15 | 3 | 5 | 2 | 630 | 1400 | 70 | 2.8 | 0.7 | 4.18 | 33.60 |
| 16 | 4 | 1 | 3 | 630 | 1400 | 98 | 0.784 | 1.47 | 5.18 | 34.42 |
| 17 | 4 | 2 | 5 | 630 | 1400 | 98 | 1.568 | 2.45 | 4.70 | 33.04 |
| 18 | 4 | 3 | 2 | 630 | 1400 | 98 | 2.352 | 0.98 | 4.94 | 34.29 |
| 19 | 4 | 4 | 4 | 630 | 1400 | 98 | 3.136 | 1.96 | 5.77 | 32.88 |
| 20 | 4 | 5 | 1 | 630 | 1400 | 98 | 3.92 | 0.49 | 4.87 | 32.74 |
| 21 | 5 | 1 | 2 | 630 | 1400 | 126 | 1.008 | 1.26 | 3.92 | 29.75 |
| 22 | 5 | 2 | 4 | 630 | 1400 | 126 | 2.016 | 2.52 | 5.80 | 27.70 |
| 23 | 5 | 3 | 1 | 630 | 1400 | 126 | 3.024 | 0.63 | 7.88 | 32.08 |
| 24 | 5 | 4 | 3 | 630 | 1400 | 126 | 4.032 | 1.89 | 8.59 | 30.31 |
| 25 | 5 | 5 | 5 | 630 | 1400 | 126 | 5.04 | 3.15 | 9.86 | 31.19 |

3.1.1. Range Analysis

Range analysis was utilized to evaluate the influence of various factors at different levels on the indicators. The *k_i* value represented the average value of the corresponding experimental results, while *R* indicated the range, which was calculated as the maximum minus the minimum for each level. A larger *R* value signifies a greater influence of that particular factor on the test results.

According to Table 3, the effects of various factors on the flexural strength of cement-based materials at 7 days were different, with the order of influence being monomer > crosslinking agent > initiator. The dosage of monomer had the greatest impact on the flexural strength of modified cement-based materials, while the effects of the initiator and crosslinking agent were similar. Similarly, for the compressive strength of cement-based materials at 7 days, the order of influence was as follows: monomer > initiator > crosslinking agent. The dosage of monomer had the greatest impact on the compressive strength of modified cement-based materials, while the crosslinking agent dosage had a minimal effect on strength. This indicated that the monomer was a significant influencing factor on the properties of modified cement-based materials, whereas initiators and crosslinking agents had similar effects.

Table 3. Range analysis results.

| | Index | Monomer A | Initiators B | Crosslinkers C |
|----------------------|-------|-----------|--------------|----------------|
| Flexural strength | k1 | 4.2 | 4.33 | 4.89 |
| | k2 | 4.07 | 4.23 | 4.45 |
| | k3 | 4.54 | 4.93 | 5 |
| | k4 | 4.95 | 5.6 | 4.4 |
| | k5 | 6.85 | 5.51 | 5.88 |
| | R | 2.78 | 1.37 | 1.48 |
| Compressive strength | k1 | 35.15 | 33.91 | 34.22 |
| | k2 | 34.77 | 32.85 | 33.62 |
| | k3 | 34.94 | 34.7 | 33 |
| | k4 | 33.47 | 35 | 32.56 |
| | k5 | 30.21 | 32.08 | 35.14 |
| | R | 4.94 | 2.92 | 2.58 |

According to the range analysis, Figures 1 and 2 illustrate corresponding index influence effect curves for each factor. Factor A represented the monomer, B represented the initiator, and C represented the crosslinking agent. There was a positive correlation between the monomer dosage and flexural strength, while there was the opposite trend for the initiator and crosslinking agent's influence on flexural strength. The optimal combination for this experiment was A5B4C5. As the monomer content increased, the compressive strength gradually decreased. With an increasing initiator content, the compressive strength initially decreased and then increased before decreasing again. With an increasing crosslinking agent content, the compressive strength showed a pattern where it first decreased and then increased. The optimal combination for this experiment was A1B4C5, which suggested that there were different correlations between monomers' impact on flexural and compressive strengths. In conclusion, only an appropriate amount of crosslinking agent and initiator can effectively enhance performance in modified materials (acrylamide in situ-polymerization-modified cement-based materials).

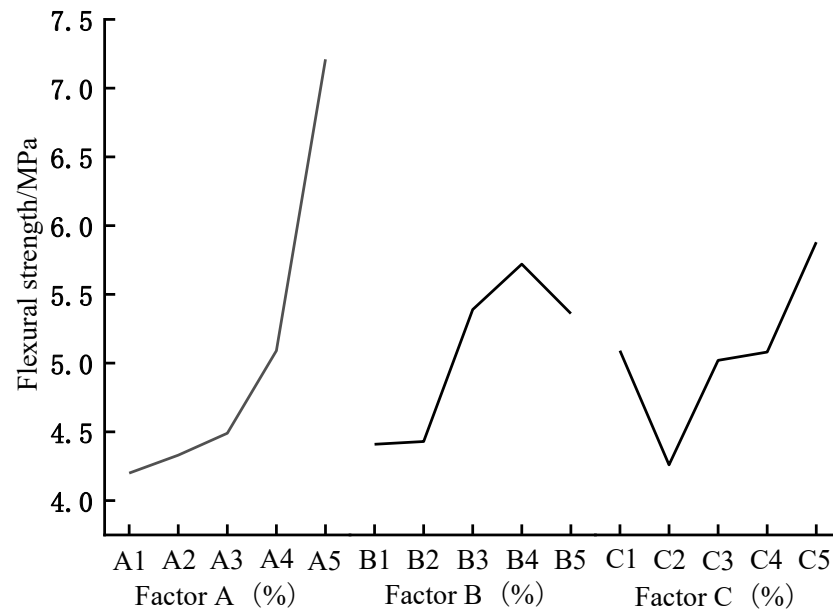


Figure 1. Flexural strengths of monomer (Factor A), initiator (Factor B), and crosslinking agent (Factor C) at each level.

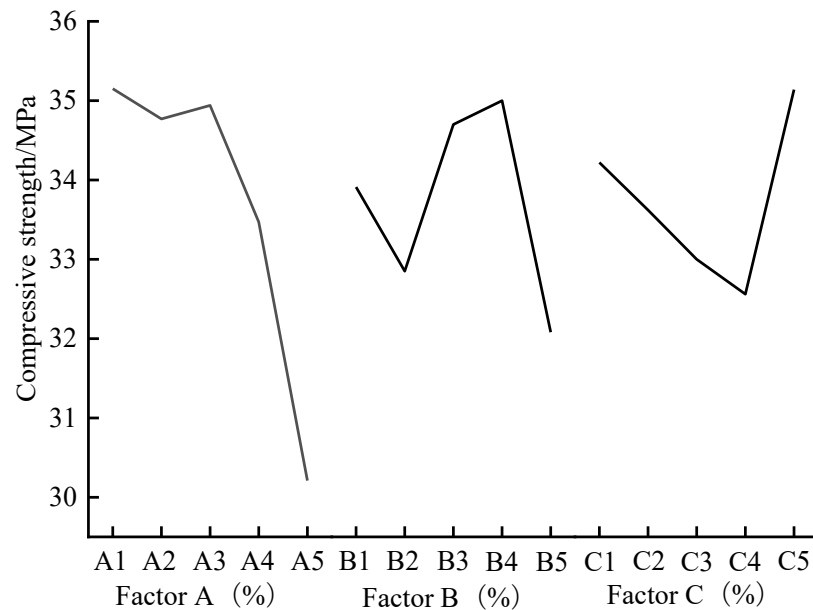


Figure 2. Compressive strengths of monomer (Factor A), initiator (Factor B), and crosslinking agent (Factor C) at each level.

3.1.2. Variance Analysis

Through analysis of variance, the significance of each factor for the experimental results was obtained, which further validated the range analysis results.

According to Table 4, the influences of various factors on flexural strength and compressive strength were different in significance. The order of significant influence of each factor on compressive strength was monomer > initiator > crosslinking agent. Similarly, the order of significant influence of each factor on flexural strength was also monomer > initiator > crosslinking agent. It can be seen from Tables 3 and 4 that the monomer was an extremely significant factor affecting the mechanical properties of polymer-modified cement-based materials.

Table 4. Variance analysis results.

| Index | Source of Variation | Deviation Squared and SS | Degree of Freedom (Df) | Mean Square Deviation (MS) | F | Significance | F0.05 | F0.01 |
|----------------------|----------------------|--------------------------|------------------------|----------------------------|-------|-----------------------|-------|-------|
| Compressive strength | Monomer A | 31.11 | 4 | 7.78 | 7.12 | Extremely significant | 3.26 | 5.41 |
| | Initiator B | 7.28 | 4 | 1.82 | 1.67 | Not significant | | |
| | Crosslinking agent C | 6.58 | 4 | 1.65 | 1.51 | Not significant | | |
| | Error e | 13.12 | 12 | 1.09 | | | | |
| Flexural strength | Monomer A | 85.20 | 4 | 21.30 | 14.92 | Extremely significant | 3.26 | 5.41 |
| | Initiator B | 30.40 | 4 | 7.60 | 5.32 | Significant | | |
| | Crosslinking agent C | 20.80 | 4 | 5.20 | 3.64 | Not significant | | |
| | Error e | 17.13 | 12 | 1.43 | | | | |

3.2. Comprehensive Scoring Method for Selecting the Optimal Ratio

The impact of each factor on the indicators was found to be consistent through both variance and range analyses. Based on the range analysis, it seemed it was possible for the optimal proportions in the experiment to be contradictory. Utilizing a comprehensive scoring method can convert multiple indicators into a single indicator for analysis in order to determine the optimal dosage, resulting in more representative test results.

In consideration of this experiment's purpose, equal importance was assigned to both indicators based on theoretical knowledge and practical experience. Therefore, a weightage value 0.5 was given to both flexural strength and compressive strength. The membership degree of each indicator was calculated, and then a comprehensive score was calculated. The comprehensive score was equal to the flexural strength membership degree \times 0.5 + compressive strength membership degree \times 0.5. The specific calculation results are shown in Table 5.

Table 5. Orthogonal design results for comprehensive scoring.

| Test No. | A | B | C | Overall Scoring |
|----------|------|------|------|-----------------|
| k1 | 0.41 | 0.37 | 0.44 | 0.41 |
| k2 | 0.40 | 0.32 | 0.34 | |
| k3 | 0.43 | 0.49 | 0.37 | |
| k4 | 0.40 | 0.53 | 0.36 | |
| k5 | 0.41 | 0.36 | 0.54 | |
| Range R | 0.02 | 0.21 | 0.20 | - |

The comprehensive scoring method was utilized to calculate the comprehensive scores of flexural strength and compressive strength. The primary influencing factor on the comprehensive index was the initiator, with secondary factors being the crosslinking agent and monomer. Range analysis was conducted based on the comprehensive score, revealing that the optimal polymer ratio was A3B4C5. The optimal ratio and the optimal combination obtained from the previous range analysis were tested and analyzed again, and the results are shown in Table 6. As shown in Table 6, the A3B4C5 combination demonstrated high compressive strength and flexural strength, thus leading to its selection as the optimal combination, with a monomer dosage of 5%, initiator dosage of 3%, and crosslinking agent dosage of 2.5%.

Table 6. Optimal combination comparison.

| Optimal Combination | Flexural Strength | Compressive Strength |
|---------------------|-------------------|----------------------|
| A1B4C5 | 4.97 | 28.68 |
| A3B4C5 | 9.55 | 36.03 |
| A5B4C5 | 5.76 | 30.44 |

3.3. Characterization

3.3.1. Fourier Transform Infrared Spectroscopy (FTIR) Analysis

The Fourier transform infrared spectrometer was utilized to compare and analyze the sulphoaluminate cement specimen (a) and polymer-modified sulphoaluminate cement specimen (b). The experimental results are presented in Figure 3.

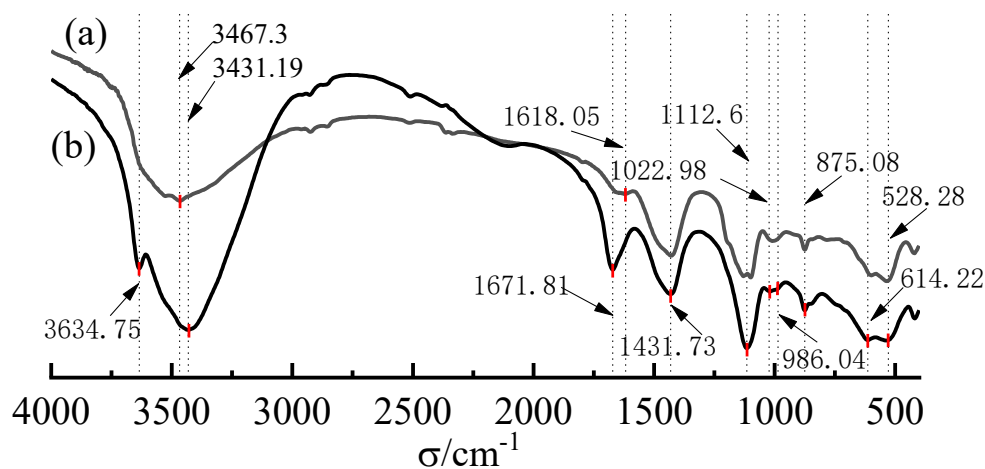


Figure 3. Infrared spectrogram of the sulphoaluminate cement specimen (a) and polymer-modified sulphoaluminate cement specimen (b).

The characteristic peak at 3467.3 cm^{-1} observed in the sulphoaluminate cement specimen can be attributed to a strong stretching vibration of O-H bonds in cement hydration product ettringite. Additionally, a minor peak at 1618.05 cm^{-1} corresponds to its bending vibration of O-H bonds. In the polymer-modified sulphoaluminate cement specimen, a new band at 3634.75 cm^{-1} appeared, indicating stretching and shrinking vibrations of N-H bonds in polymers. Furthermore, a relatively intense absorption peak at 3431.19 cm^{-1} was observed due to stretching vibrations of O-H bonds in cement hydration product ettringite. The polymer-modified sulphoaluminate cement specimen exhibited a significant C=O stretching vibration peak for carboxylate ions at 1671.81 cm^{-1} and a C-O stretching vibration at 1431.73 cm^{-1} , suggesting that monomers undergo polymerization reactions leading to polymer formation. Compared with the sulphoaluminate cement specimen's peak width, there was decreased intensity for the $[\text{SO}_4^{2-}]$ (a hydration product of ettringite) stretching vibration phase observed at 1115.7 cm^{-1} . Moreover, the N-H vibrational peak shifted towards lower wavenumbers (1022.98 cm^{-1}), providing evidence of new chemical bond formation between cement hydration products and polymers. Peaks near 900 cm^{-1} and 500 cm^{-1} could be ascribed to bending and stretching vibrations of Si-O and Al-O bonds, respectively.

Based on the comprehensive analysis above, it can be seen that the monomer acrylamide was in situ-polymerized in the cement-based material to form a polymer. At the same time, a new network structure was formed between the polymers and cement hydration products. This network structure improved the compatibility and stability of cement-based materials.

3.3.2. X-ray Diffraction (XRD) Analysis

The X-ray diffractometer utilizes X-ray irradiation to induce diffraction phenomena, and a graph is generated based on the signal detected by the instrument. Through wave-form analysis, peak intensity measurement, and peak position determination, characteristic information of the sample can be obtained.

The sulphoaluminate cement specimen was used as the benchmark group, and the polymer-modified sulphoaluminate cement specimen was used as the polymer modification group. According to Figure 4, the XRD patterns of both the polymer modification group and benchmark group after 7 days of curing reveal a prominent Aft diffraction peak. This indicates that the main hydration product in cement was Aft, with a small amount of hydrated calcium silicate gel present. There was no significant difference in hydration products between the benchmark group and polymer modification group. Moreover, no new hydration products were observed in polymer-modified cement-based materials compared to the benchmark group.

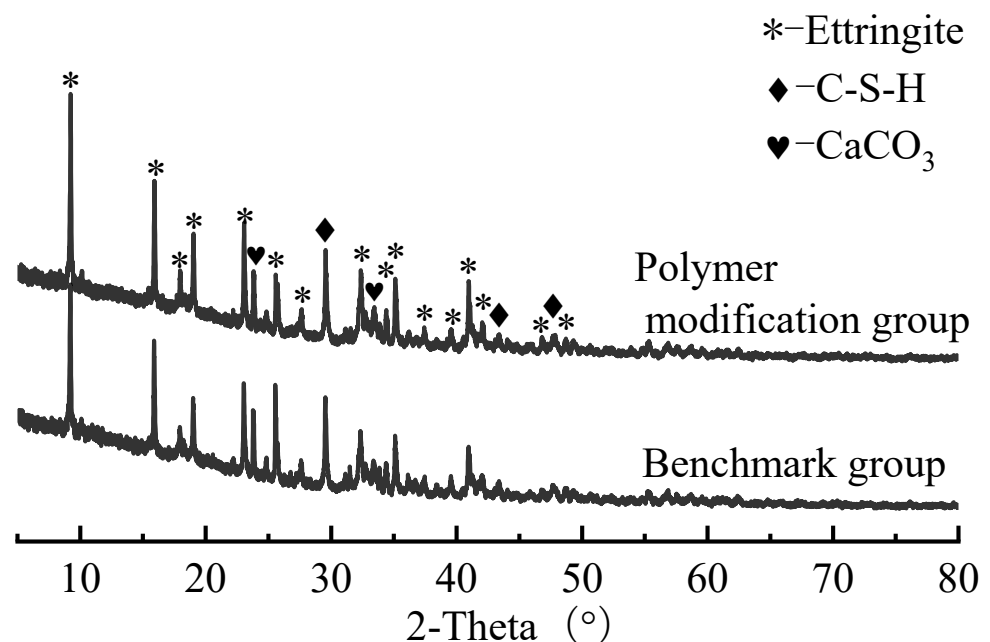


Figure 4. XRD patterns of polymer modification group and benchmark group.

3.3.3. Field Emission Scanning Electron Microscopy (SEM) Analysis

After 7 days of curing, SEM testing was conducted on both specimens: (a) the sulphoaluminate cement specimen and (b) polymer-modified sulphoaluminate cement specimen, with the results shown in Figure 5. Photos of these specimens are presented in Figure 6. When comparing SEM images under $5000\times$ magnification (Figure 5), it can be observed that there was a distinct disparity between the sulphoaluminate cement specimen (a) and polymer-modified sulphoaluminate cement specimen (b). In case of the sulphoaluminate cement specimen (a), loose rigid network structures consisting of numerous needle-shaped ettringite crystals, rod-shaped ettringite crystals, and reticular gel were formed as hydration products. Additionally, there were obvious micro-cracks and cracks on the surface of cement hydration products. A large amount of ettringite was exposed in the spatial structure, and the connection with the hydrated gel material was not tight, resulting in poor structural compactness of the material.

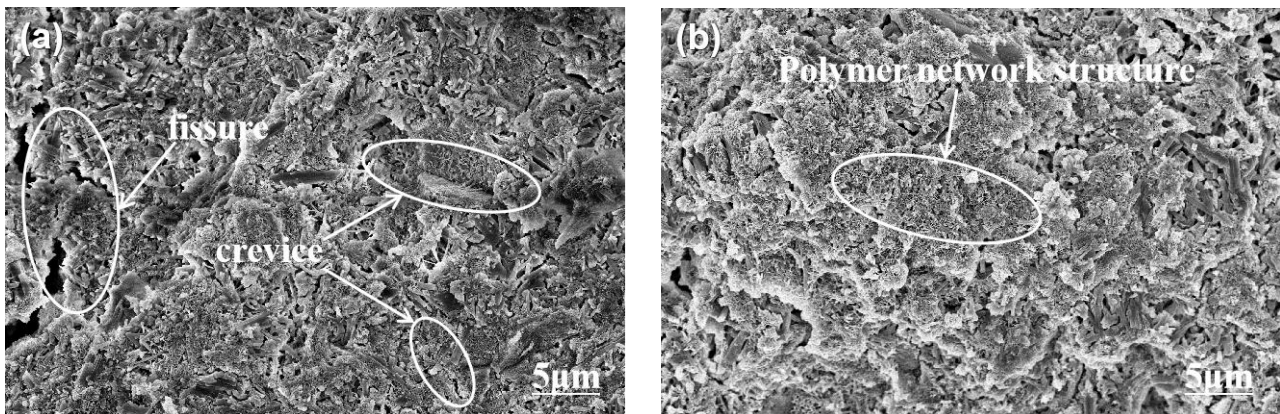


Figure 5. SEM images of the sulphoaluminate cement specimen (a) and polymer-modified sulphoaluminate cement specimen (b).

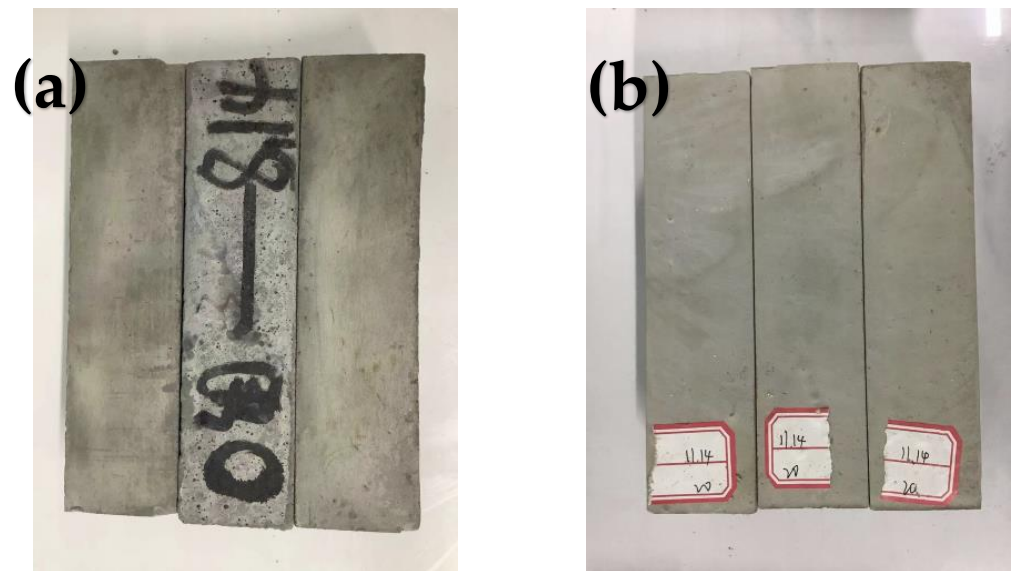


Figure 6. Photos of the sulphoaluminate cement specimen (a) and polymer-modified sulphoaluminate cement specimen (b).

On the contrary, in the case of the polymer-modified sulphoaluminate cement specimen, acrylamide formed a network structure via in situ polymerization, which interpenetrated with rigid structures formed by cement hydration, leading to the formation of a dense double network structure. The material exhibited an absence of obvious cracks, and there was a minimal space leakage phenomenon for ettringite, indicating its close connection with gel materials as well as polymers.

By combining FT-IR, XRD, and SEM analysis, it can be concluded that the in situ polymerization of acrylamide resulted in the formation of a more stable network structure with the cement hydration product. The amide groups of the polymer exhibited strong reactivity, while the hydrolyzed -COOH- groups demonstrated significant adsorption ability and reacted with ions in cement hydration products. The carboxyl group reacted and became fixed, leading to a relatively stable structure formed by polymers and cement hydration products. Compared to the sulphoaluminate cement specimen group, polymer-modified cement-based materials showed improved material properties. The in situ polymerization of acrylamide led to the formation of an organic macromolecular polymer, which intertwined, penetrated, and condensed with the spatial network structure formed by polymers and cement hydration products to create a complex three-dimensional network structure. This polymer wrapped around ettringite surfaces as well as hydrated

gel materials while filling cracks and structural gaps within cement stone. Its network structure exhibited excellent compatibility with cement-based materials due to its adhesion properties through new chemical bonds formed between cement hydration products. Furthermore, this three-dimensional spatial network structure demonstrated high density, compatibility, and adhesion characteristics. This study provides a theoretical foundation for enhancing our knowledge of macroscopic properties.

4. Conclusions

Acrylamide in situ-polymerization-modified cement-based materials represent a novel type of modified material that can effectively enhance the performance of cement-based materials, which holds significant implications for harbor engineering research. This approach offers an efficient method for achieving high-performance and functionalized cement-based materials.

- (1) According to the orthogonal experiment, the monomer was found to be a significant influencing factor for the performance of modified cement-based materials. The optimal preparation dosages of polymer-modified cement-based materials were as follows: monomer 5%, initiator 3%, and crosslinking agent 2.5%.
- (2) Structural characterization revealed that in situ polymerization of acrylamide formed a network polymer structure that intersected with and penetrated the rigid spatial skeleton structure formed by cement hydration products, leading to an organic–inorganic dual network structure. The polymer served as both filler and binder without altering the composition of cement hydration products. However, stable chemical bonds were established between these products and polymers. This improvement significantly enhanced the density and stability of polymer-modified cement-based materials, preparing them for subsequent marine performance research.

Author Contributions: Conceptualization, X.F.; methodology, X.F.; software, B.L.; validation, X.F.; formal analysis, X.F.; investigation, B.L.; resources, B.L.; data curation, B.L.; writing—original draft preparation, X.F.; writing—review and editing, X.F. and B.L.; visualization, B.L.; supervision, X.F.; project administration, X.F.; funding acquisition, X.F. All authors have read and agreed to the published version of the manuscript.

Funding: This work was supported by Hainan Natural Science Foundation High-level Talent Project [Grant No. 521RC1035].

Institutional Review Board Statement: Not applicable.

Informed Consent Statement: Not applicable.

Data Availability Statement: The original contributions presented in the study are included in the article, further inquiries can be directed to the corresponding author.

Conflicts of Interest: The authors declare no conflicts of interest.

References

1. Su, F.Y.; Wang, H.Y.; Ma, X.D. Review of the Influence of Acrylate Lotion on the Properties of Cement-Based Materials. *Materials* **2023**, *16*, 6597. [[CrossRef](#)] [[PubMed](#)]
2. Wang, M.; Chen, N. Preparation of Trilobal Poly Fiber and Its Reinforcement for Cement-based Composite Materials. *Polym. Mater. Sci. Eng.* **2020**, *36*, 275–279.
3. Bahranifard, Z.; Tabrizi, F.F.; Vosoughi, R.A. An investigation on the effect of styrene-butyl acrylate copolymer latex to improve the properties of polymer modified concrete. *Constr. Build. Mater.* **2019**, *20*, 175–185. [[CrossRef](#)]
4. Fan, L.D.; Xu, F.; Wang, S.R. A review on the modification mechanism of polymer on cement-based materials. *J. Mater. Res. Technol.* **2023**, *26*, 5816–5837. [[CrossRef](#)]
5. Xu, Y.C.; Xing, G.H.; Hang, J.L. Effect of PVA Fiber and Carbon Nanotubes Modification on Mechanical Properties of Concrete. *J. Build. Mater.* **2023**, *26*, 809–815.
6. Liu, F.; Wang, B.M.; Yuan, X.S. Experimental analysis on mechanical properties and durability of cement concrete modified by styrene-butadiene latex. *J. Funct. Mater.* **2019**, *50*, 6167–6173.

7. Jin, H.S.; Li, F.H.; He, X. Research on Frost Resistance of Polypropylene Fiber Cement-based Composite Material. *Mater. Rev.* **2020**, *34*, 71–76.
8. Li, L. Study on the Influence and Mechanism of Nano Organic and Inorganic Hybrid Materials on Cement Hydration. Ph.D. Thesis, Chongqing University, Chongqing, China, 2020.
9. Abu, T.; Ala, S.; Ghassan, S.; Senouci, A. Using Aerosol OT in Hexane Solution to Synthesize Calcium Nitrate Self-Healing Refined Microcapsules for Construction Applications. *Buildings* **2022**, *12*, 751. [[CrossRef](#)]
10. Yin, B.; Hau, X.L.; Qi, D.M. Multi-scale synergistic modification and mechanical properties of cement-based composites based on in-situ polymerization. *Cem. Concr. Compos.* **2023**, *137*, 104945. [[CrossRef](#)]
11. Zhou, Z.H.; Lin, Z.F.; Gao, X.J. Study on properties of Portland cement-sulfoaluminate cement-based grouting materials modified by in-situ polymerization of calcium acrylate. *Constr. Build. Mater.* **2023**, *409*, 175–185. [[CrossRef](#)]
12. Wang, Z.M.; Cai, Y.Y.; Zhang, L. Study on properties and mechanism of interpenetrating network structure cementitious composites. *Concrete* **2021**, *11*, 70–74.
13. Liu, Q.; Liu, W.; Li, Z.; Guo, S.; Sun, G. Ultra-lightweight cement composites with excellent flexural strength, thermal insulation and water resistance achieved by establishing interpenetrating network. *Constr. Build. Mater.* **2020**, *250*, 118923. [[CrossRef](#)]
14. He, R.; Zheng, X.X.; Wang, Y. Research status of properties and modification technology of sulphoaluminate cement. *Appl. Chem. Ind.* **2022**, *51*, 1495–1501.
15. Niu, M.; Li, G.; Wang, Y. Comparative study of immobilization and mechanical properties of sulfoaluminate cement and ordinary Portland cement with different heavy metals. *Constr. Build. Mater.* **2018**, *19*, 333–343. [[CrossRef](#)]
16. Liu, Z.X.; Wang, L.B. *Experimental Design and Data Processing*; Chemical Industry Press: Beijing, China, 2020; pp. 66–79.
17. GB/T 17671-2021; Test Method of Cement Mortar Strength (ISO Method). China Standards Press: Beijing, China, 2021; pp. 12–13.

Disclaimer/Publisher’s Note: The statements, opinions and data contained in all publications are solely those of the individual author(s) and contributor(s) and not of MDPI and/or the editor(s). MDPI and/or the editor(s) disclaim responsibility for any injury to people or property resulting from any ideas, methods, instructions or products referred to in the content.